Polymer 50 (2009) 1986–2000

Contents lists available at ScienceDirect

Polymer

journal homepage: www.elsevier.com/locate/polymer

ATRP poly(acrylate) star formation: A comparative study between MALDI and ESI mass spectrometry

Gene Hart-Smith [a,b], Mieke Lammens [c], Filip E. Du Prez [c,*], Michael Guilhaus [b], Christopher Barner-Kowollik [a,**]

[a] Preparative Macromolecular Chemistry, Institut für Technische Chemie und Polymerchemie, Universität Karlsruhe (TH)/Karlsruhe Institute of Technology (KIT), Engesserstraße 18, 76128 Karlsruhe, Germany
[b] UNSW Analytical Centre, Chemical Sciences Building, The University of New South Wales, Sydney, NSW 2052, Australia
[c] Ghent University, Department of Organic Chemistry, Polymer Chemistry Research Group (PCR), Krijgslaan 281 S4-bis, B-9000 Ghent, Belgium

ARTICLE INFO

Article history:
Received 8 January 2009
Received in revised form
27 February 2009
Accepted 5 March 2009
Available online 18 March 2009

Keywords:
Mass spectrometry
Atom transfer radical polymerisation (ATRP)
Star polymers

ABSTRACT

Optimised matrix-assisted laser desorption/ionisation (MALDI) and electrospray ionisation (ESI) mass spectrometry (MS) methodologies were systematically compared in terms of their relative abilities to identify distinct chemical species present in samples associated with a polymer mechanistic study. In order to perform the investigation, formation processes involved in atom transfer radical polymerisation (ATRP) mediated methyl acrylate (MA) star polymerisations were studied. In addition to the 4-armed ATRP initiator employed in the polymerisations, initiator side-products were found to generate oligomeric chains. At a relatively high monomer to polymer conversion, terminal Br loss was observed in these oligomers; this Br loss was hypothesised to occur via degradative transfer reactions involving the radicals $(CH_3)_2\dot{C}OH$, $\dot{C}H_3$ and $\dot{C}H_2COCH_3$, which were derived from the acetone used as a solvent in the polymerisations, as well as hydrogen radicals donated by the ligand *N*,*N*′,*N*′,*N*″,*N*″-pentamethyldiethylenetriamine (PMDETA). In performing these studies, ESI was found to identify a greater number of distinct chemical species in the samples under investigation when compared to the employed MALDI technique, suggesting that the utilisation of ESI must be strongly considered in polymer mechanistic investigations if the maximum number of end-group functionalities within a given polymer sample are to be identified.

© 2009 Elsevier Ltd. All rights reserved.

1. Introduction

In the characterisation of synthetic polymers, mass spectrometry (MS) has been demonstrated to be an exceptionally powerful analytical method. Particularly since the development of soft ionisation techniques such as matrix-assisted laser desorption/ionisation (MALDI) and electrospray ionisation (ESI), MS has garnered increasing attention in the field of polymer chemistry to the point of being considered a standard analytical tool. Much of the early attention was focused upon applying these soft ionisation techniques towards the direct analysis of molecular weight distributions (MWDs) [1], but it has since become clear that mass discrimination effects that can occur during the ionisation, transmission and detection phases of a given MS experiment restrict the ability to obtain accurate MWD data [2], and the accuracy of such data can only be guaranteed via coupling with size exclusion chromatography (SEC) [2,3]. However, for investigations into the mechanisms of polymerisation processes, the power of MS has become increasingly apparent. Unlike other techniques that have commonly been applied to the analysis of synthetic polymers, such as SEC and nuclear magnetic resonance (NMR) spectroscopy, MS allows absolute molecular weight information to be accessed for the individual polymer chains present within a given sample. This provides a unique and potent means by which polymer end-group functionalities can be characterised, allowing insights to be gained into the reaction pathways of a given polymerisation. Indeed, the utility of such MS techniques in polymer mechanistic studies has been well documented in recent review articles [4,5].

To date, the majority of MS based studies on synthetic polymers have been conducted using MALDI instruments [1,2,4–7]. A reason for this is that the time-of-flight (TOF) mass analysers to which MALDI sources are generally interfaced are amenable to the

* Corresponding author. Tel.: +32 9 264 4503; fax: +32 9 264 4972.
** Corresponding author. Tel.: +49 721 608 5641; fax: +49 721 608 5740.
E-mail addresses: filip.duprez@ugent.be (F.E. Du Prez), christopher.barner-kowollik@polymer.uni-karlsruhe.de (C. Barner-Kowollik).

0032-3861/$ – see front matter © 2009 Elsevier Ltd. All rights reserved.
doi:10.1016/j.polymer.2009.03.009

analysis of high mass-to-charge ratios (m/z), allowing polymers to be analysed into the Mega Dalton mass range [8]. On the other hand, the m/z amenable to analysis on ESI mass spectrometers is generally more restricted due to the common implementation of quadrupole mass analysers in these instruments, and polymers of a mass beyond this limited range are unable to be observed unless they are detected as multiply charged ions. Additionally, the formation of such multiply charged ions in MALDI is generally less prevalent than in ESI. This can be an important consideration, as extensive multiple charging of ions can render mass spectra difficult or even impossible [9] to interpret. Despite these often claimed advantages of MALDI instruments over ESI instruments, there are numerous other instrumental characteristics that are of pertinence to a successful MS based polymer mechanistic study. These characteristics include the mass resolving power and mass accuracy capabilities of the instrument employed in a given study; the relative propensity for end-group fragmentation to occur in an instrument interfaced with a given ionisation source; and the ability of an instrument to detect a wide dynamic range of product abundances within a polymer sample. For instance in a polymer sample with differing end-group functionalities of disparate abundances, the signal-to-noise ratios (S/N) obtained for ions formed from these different products will determine whether or not these species can be identified via MS, and hence whether or not the reaction pathways associated with these products can be elucidated. How a specific MALDI or ESI instrument relates to these considerations will not only be dependent upon the ionisation source employed, but also on the mass analyser and detector interfaced to the instrument in question.

Despite there being numerous important factors that must be considered when deciding upon the instrumentation to be used in a particular polymer mechanistic investigation, these factors have rarely been systematically compared for ESI and MALDI instruments in the analysis of synthetic polymers. Of the comparative MALDI and ESI studies that have been conducted, most have focused upon how observed MWDs compare for specified polymer systems when using instruments featuring these different ionisation modes [10–14]. There has also been some research into how signal intensities for distinct end-group functionalities or polymer architectures within a given polymer system differ when analysed using instruments interfaced with MALDI or ESI ionisation sources [11,14,15]. Only very recently has attention been focused upon the comparative abilities of MALDI and ESI instruments to comprehensively identify distinct products present in polymer samples; for the specific MS instruments and sample preparation techniques used in their study, Ladaviére et al. found that ESI was able to identify a greater number of end-group functionalities than MALDI in poly(styrene) samples synthesised via a variety of controlled radical polymerisation (CRP) protocols [16]. In order to allow the choice between MALDI and ESI to be made with a greater degree of knowledge, in this study we aim to extend these investigations by systematically comparing the abilities of MALDI and ESI instruments to comprehensively identify the distinct products present in samples associated with a mechanistic investigation involving polymers synthesised using methyl acrylate (MA).

In order to compare the performances of instruments implementing these two physically dissimilar ionisation processes, MA star polymers mediated via atom transfer radical polymerisation (ATRP) were chosen in part for their amenability towards analysis via the ionisation techniques of interest. Indeed, mechanistic studies upon poly(MA) systems have been successfully undertaken in the past using both MALDI [17–19] and ESI [20–24]. Additionally, the ATRP star polymer system under scrutiny has the capability of displaying a high degree of end-group complexity due to the potential for events such as star–star coupling [25] and mid-chain radical (MCR) formation [22], making the system ideally suited to a detailed mechanistic investigation. To increase the scope of the study with regards to its practical applicability, we will focus upon the use of frequently employed commercially available instrumentation, and on the optimisation of the most commonly utilised sample preparation techniques. Clearly such limitations cannot allow a definitive answer to be given to the broad question of which ionisation protocol is better suited to the comprehensive identification of end-group functionalities that are present in polymer samples at highly disparate abundances. However, the study provides another reference point for the furthering of this discussion, and points towards an answer to this question for a wide range of polymer mechanistic investigations.

2. Experimental section

2.1. Materials

2,2-Bis(hydroxymethyl)propionic acid (bis-MPA, Aldrich, 98%), 2-bromo-2-methylpropionyl bromide (Aldrich, 98%), 1,4-benzenedimethanol (Acros, 99%), *N*,*N*′-dicyclohexylcarbodiimide (DCC, Aldrich, >99%), 4-(dimethylamino)pyridine (DMAP, Aldrich, >99%), acetone (Aldrich, HPLC grade), dichloromethane (DCM, Aldrich, HPLC grade), methanol (Ajax Chemicals, HPLC grade), *trans*-2-[3-(4-*tert*-butylphenyl)-2-methyl-2-propenylidene]malononitrile (BMPM, Aldrich, 99%) and trifluoroacetic acid potassium salt (Acros Organics, 98%) were used as received. Cu(I)Br (Aldrich, 98%) was purified by being stirred in acetic acid, followed by filtration, washing with methanol, and drying in a vacuum oven at 70 °C. *N*,*N*′,*N*′,*N*″,*N*″-Pentamethyldiethylenetriamine (PMDETA, Acros, >99%) and methyl acrylate (MA, Aldrich, >99%) were distilled under reduced pressure.

2.2. Initiator precursor synthesis

2-Bromo-2-methylpropionyl bromide (357 mmol) was added dropwise to a solution of bis-MPA (structure 1 of Scheme 1, 149 mmol, 298 equiv of OH), and dry triethylamine (366 mmol) in 500 mL of dry dichloromethane at 0 °C under argon atmosphere. After stirring at 0 °C for 1 h, the reaction was completed by stirring for another 2 h at 25 °C. Following this, the solvent was evaporated, the residue dissolved in diethyl ether and the triethylamine hydrochloride was filtered off. The solution was extracted with 2 N hydrochloride, the ether phase dried over $MgSO_4$ and the solvent evaporated to give a viscous liquid. To remove all of the 2-bromo-2-methylpropionic acid byproduct (singlet at 1.89 ppm in ^{1}H NMR), the residue was stirred with hot water several times and re-dissolved in diethyl ether. The diethyl ether was dried and evaporated, and the crude product was recrystallised from hexane to give the product as a white solid.

2.3. Initiator synthesis

1,4-Benzenedimethanol (0.2911 g) and the precursor (structure 2 of Scheme 1, 1.1 equiv with respect to OH groups) were dissolved in ca. 7 mL of dichloromethane. To this, 1.3020 g DCC (1.5 equiv) and 0.1302 g DMAP (10 wt% relative to DCC) were added, and the solution was stirred overnight at room temperature. The solution was filtered to remove the urea byproduct and the product (structure 3 of Scheme 1) purified by repeated column chromatography (silica gel, hexane/ethyl acetate 4:1). 500 MHz ^{1}H NMR ($CDCl_3$): δ [ppm] = 1.35 (s, 6H, CH_3), 1.87 (s, 24H, CH_3–CBr), 4.33–4.44 (m, 8H, CH_2), 5.16 (s, 4H, CH_2–Ar), 7.34 (s, 4H, Ar*H*).

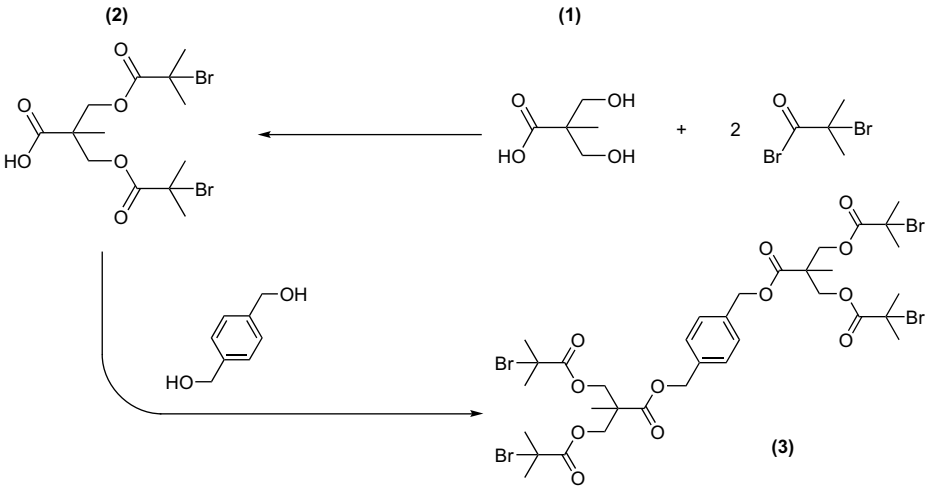

Scheme 1. The procedure used to synthesise the 4-armed ATRP initiator used in the generation of star-shaped poly(MA).

2.4. Polymerisation procedure

In a typical polymerisation, the initiator was dissolved in acetone, followed by the addition of MA and then PMDETA (2 equiv). The mixture was degassed by 3 freeze–pump–thaw cycles and the catalyst Cu(I)Br (2 equiv) added under a constant nitrogen flow. The mixture was stirred at room temperature for 15 min and the reaction flask immersed in an oil bath thermostated at 50 °C for the duration of the polymerisation. The polymerisation process was ended by cooling the reaction mixture in liquid nitrogen. The reaction mixture was diluted in THF, and the copper removed by passing the diluted mixture over a neutral Al_2O_3 column. The solvent was evaporated off and the polymer dried under vacuum.

2.5. ^1H NMR

Spectra were recorded in $CDCl_3$ at room temperature on a Bruker AM500 spectrometer at 500 MHz or on a Bruker Advance 300 at 300 MHz.

2.6. MALDI–MS

MALDI mass spectra were recorded on an Applied Biosystems Voyager DE STR MALDI–TOF spectrometer (Applied Biosystems, Nieuwerkerk ad Ijssel, the Netherlands) equipped with 2 m linear and 3 m reflecting flight paths and a 337 nm nitrogen laser (3 ns pulse). All mass spectra were obtained with an accelerating potential of 20 kV in positive ion mode and in reflector mode. Typically, the data from approximately 250 shots were signal averaged to obtain a final spectrum [26]. A poly(ethylene oxide) standard (M_n 2000 g mol^{-1}) was used for calibration. All data were processed using the Data Explorer (Applied Biosystems) and the Polymerix (Sierra Analytics) software packages.

An optimised dried droplet method [27] was used during preparation of initiator and polymer samples for MALDI analysis (see Section 3.1.1 for further elaboration). For both the initiator and polymer samples, it was found that optimal results were achieved if BMPM (20 mg/mL in THF) was used as the matrix, trifluoroacetic acid potassium salt (1 mg/mL) was used as the cationating agent, and samples were dissolved in THF (2 mg/mL). Analyte solutions were prepared by mixing 10 μL of the matrix, 5 μL of the salt, and 5 μL of the analyte. Subsequently, 0.5 μL of this mixture was spotted on the sample plate, and the spots were dried in air at room temperature.

2.7. ESI-MS

ESI mass spectra were recorded on a Thermo Finnigan LCQ Deca ion trap mass spectrometer (Thermo Finnigan, San Jose, CA). The LCQ Deca ion trap instrument was equipped with an atmospheric pressure ionisation source operating in the nebuliser assisted electrospray mode and was used in positive ion mode. Mass calibration was performed using caffeine, MRFA and Ultramark 1621 (Aldrich) in the m/z range 195–1822 Da. All spectra were acquired within the m/z range of 150–2000 Da, and typical instrumental parameters were a spray voltage of 4.5 kV, a capillary voltage of 44 V, a capillary temperature of 275 °C and a flow rate of 3.50 μL/min. Nitrogen was used as sheath gas (flow: 50% of maximum) and helium was used as auxiliary gas (flow: 5% of maximum). 3 microscans, with a maximum inject time of 100 ms per microscan, were averaged for each scan when using the normal scan type. When using the *ZoomScan* scan type, 5 microscans were averaged per scan, with a maximum inject time of 50 ms per microscan. For each respective scan type, approximately 350 scans were signal averaged to obtain the final spectrum [26].

Tandem MS (MS/MS) experiments were conducted upon precursor ions of interest using identical source conditions to non-tandem MS experiments. Helium collision gas was used at a partial pressure of 0.1 Pa, and typical normalised collision energies ranged from 25 to 45%.

Optimised spectral quality was obtained when a 75/25 vol% mixture of dichloromethane (DCM)/methanol (MeOH) was used as the solvent mixture and ca. 5 mg/mL of analyte was added. No supplementary cation addition was required for optimal results to be obtained (see Section 3.1.2 for further elaboration).

2.8. Mass analysis

Products produced during the ATRP MA star polymerisations were identified by assigning chemical structures to the ions detected during the ESI-MS and MALDI–MS analyses. In order to aid in the identification of these ions, a structural library was created for the possible products generated in the star polymer system

under investigation (see Section 3.2 for further elaboration). All theoretical monoisotopic molecular weights were calculated using the exact mass as provided by the software package CS ChemDraw Ultra® version 5.0 for the lightest isotope of the product of interest. Theoretical isotopic peak patterns were generated using the software package Xcalibur™ version 1.4.

3. Results and discussion

The MALDI and ESI conditions employed in the present study are discussed below, followed by a discussion of the structural library created for the ATRP MA star polymer system under investigation. MS analyses are then presented for three different samples

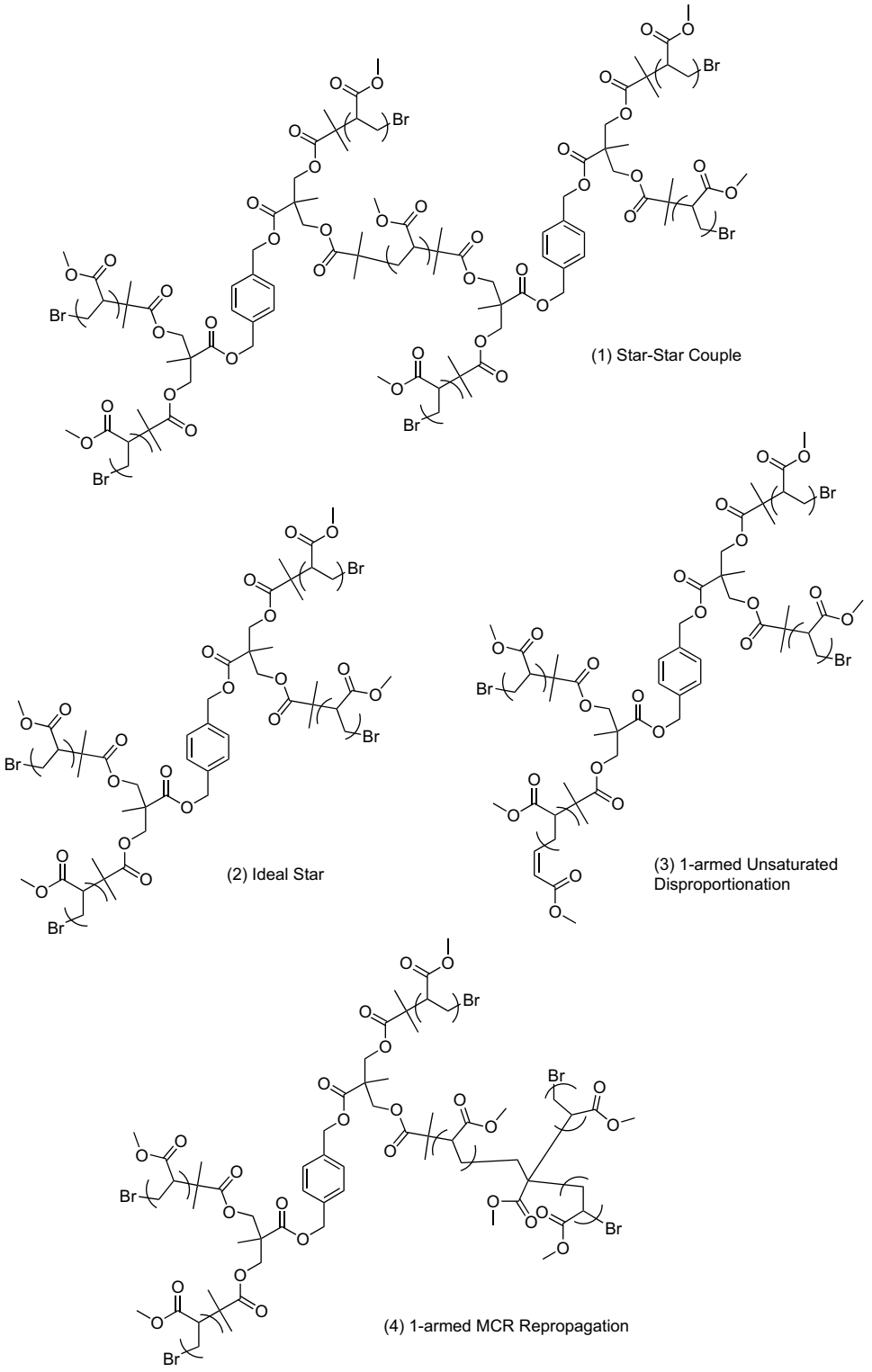

Scheme 2. Examples of chemical structures incorporated into the structural library. Repeating monomer units have been enclosed with brackets. Due to the high number of structures incorporated into the library, only a limited number of illustrative examples have been shown.

associated with the current mechanistic investigation: the 4-armed ATRP initiator, a lower conversion star poly(MA) sample and a higher conversion star poly(MA) sample. For each of these samples, the respective MALDI and ESI data are presented, along with any insights gained from the data. Finally the overall performances of the MALDI and ESI-MS analyses are compared, with an emphasis upon the relative ability of each technique to provide detailed identification of the distinct products present within the samples under investigation.

3.1. Mass spectrometry conditions

In order to successfully compare the relative abilities of the MALDI and ESI instruments employed in the present study to detect analyte molecules of disparate abundances within a given sample, it was imperative to obtain optimised data from each instrument. For our purposes optimal MS conditions involved allowing the maximum number of analyte ions to be detected using a given MS technique, which largely concerned maximising the *S*/*N* of these ions. The considerations that were made when optimising each ionisation technique are outlined below.

3.1.1. MALDI–MS

When considering MALDI-TOF mass spectrometers, it is useful to note that the capability for TOF mass analysers to measure substantially differing analyte signals is generally restricted by the limited dynamic range (1–255) of the available high speed analog-to-digital converters (ADC) used in the instrument detection systems [28]. However these limitations are rarely reached when polymer samples are analysed via MALDI; rather, the ability to detect lower abundance ions from a polymer sample is generally restricted by the level of chemical noise [29], which is largely determined by the method of sample preparation.

One of the most influential factors in the preparation of samples for analysis via MALDI is the selection of the matrix. Though general guidelines for matrix selection in the preparation of polymer samples were taken into consideration [30,31], our process of matrix selection remained largely trial and error. Furthermore, although numerous attempts have been made to improve MALDI sample preparation techniques; such as methods of accelerated crystallisation [32–34], spin coating [35], the thin layer method [36] and electrospray deposition [37–40]; the traditional dried droplet technique [27] still predominates in polymer analyses due to its simplicity and lack of a need for specialised equipment. As outlined

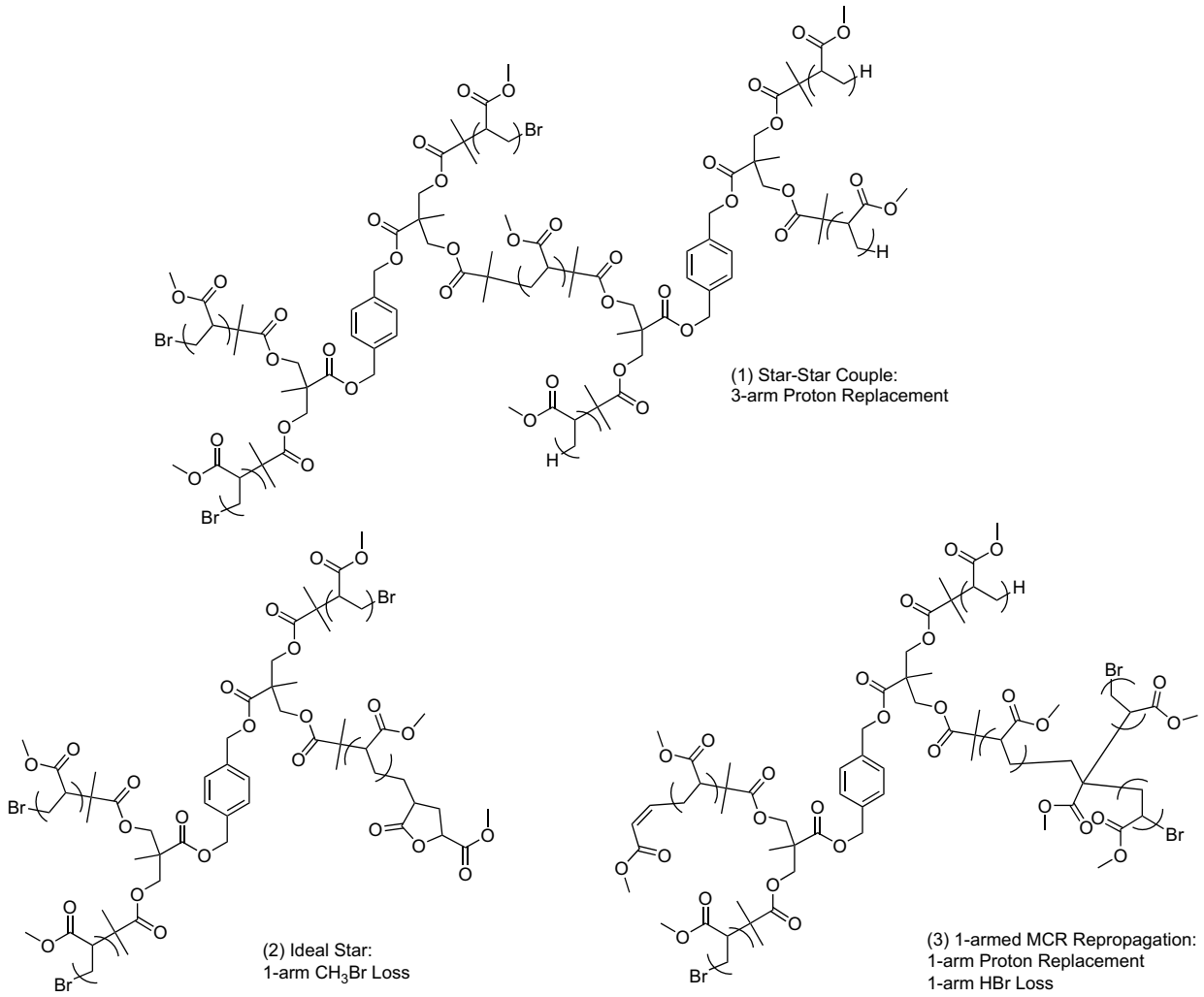

Scheme 3. Examples of chemical structures incorporated into the structural library. Such structures are associated with the elimination of terminal bromine functionalities. Repeating monomer units have been enclosed with brackets. Due to the high number of structures incorporated into the library, only a limited number of illustrative examples have been shown.

in Section 1, the most commonly implemented sample preparation techniques were chosen for this study in order to ensure that the scope of the investigation remained broad; therefore through a trial and error investigation of different matrix, salt and solvent combinations, the dried droplet technique was optimised for the analyses of the samples under investigation (see Section 2.6 for the optimised sample preparation technique).

3.1.2. ESI-MS

Like MALDI instruments, the ability for ESI mass spectrometers to detect lower abundance ions from a polymer sample is predominantly restricted by chemical noise. For ESI, both the sample preparation and the choice of analytical conditions will have a significant effect on the observation of such chemical noise.

When optimising the parameters associated with sample preparation, it was noted that the choice of solvent, analyte concentration, and the nature and concentration of any added cations will all have an impact upon the ionisation and desorption efficiency, and the *S*/*N* of observed ions [11]. With regards to the analytical conditions employed in the ESI analyses, parameters including the flow rate of the nebulising gas and the solvent flow rate were considered [41]. All of these parameters influence the propensity for analyte ions to be released into the gas phase from the electrically charged droplets formed during the electrospray process, and these parameters were systematically altered when optimising the MS conditions for each of the samples under investigation (see Section 2.7 for the optimised MS conditions).

3.2. Structural library

To aid in the assignment of chemical structures to the ATRP star poly(MA) system under investigation from the optimised mass spectra, a comprehensive structural library containing products potentially generated during the polymerisations was created (see Schemes 2 and 3 for examples of these structures). These products include ideal star molecules (structure (2) of Scheme 2), products with star arms terminated via intermolecular or intramolecular combination reactions (e.g. structure (1) of Scheme 2) [25,42], and products with star arms terminated via disproportionation reactions (e.g. structure (3) of Scheme 2). Chemical structures likely to be generated as a consequence of mid-chain radical (MCR) formation were also included in the library [22]. Products associated with β-scission, termination by both disproportionation and combination, and re-propagation (e.g. structure (4) of Scheme 2) of these MCRs were included. Additionally, for each of the aforementioned chemical structures with bromine end-group functionalities, the elimination of terminal bromine via HBr loss (e.g. structure (3) of Scheme 3) [43], CH_3Br loss (e.g. structure (2) of Scheme 3) [44] or proton replacement (e.g. structures (1) and (3) of Scheme 3) [17,43,45–47] was considered.

For every compound incorporated into the structural library, the masses of adducts formed from these compounds via the attachment of various different cations were calculated ($[P+(M)_n]^{n+}$, where P represents an analyte molecule; M represents sodium, potassium, lithium, silver, hydrogen or ammonium cations; and $n=1$ for singly charged ions or $n=2$ for doubly charged ions). The exact masses calculated for these adduct species were used in the assignment of peaks generated in the MS experiments. The masses of various salt cluster complexes ($[P+M(MX)_m]^{n+}$, where MX represents the metal salt and M the metal cation; m and $n=1$ or 2) were also taken into consideration.

3.3. Initiator MS analysis

The following section presents MALDI and ESI data obtained from the ATRP initiator sample. In addition to the main 4-armed ATRP initiator product (structure 3 of Scheme 1), it was deemed feasible that lower abundance side-products remaining from the initiator synthesis could also be present within the sample. ^{1}H NMR data obtained from the sample lent support to this hypothesis (see Fig. S1 of the Supplementary data). As any terminal bromine containing side-products could feasibly also initiate polymerisations, and thus complicate the resulting product distributions of poly(MA) samples, a thorough examination of the initiator sample for such side-products plays an important role in the present mechanistic investigation.

3.3.1. MALDI–MS results

The upper portion of Fig. 1 shows a typical mass spectrum obtained from the initiator sample via MALDI. The spectrum is complicated by the presence of abundant matrix ion signals in the lower *m*/*z* regions, making the identification of sample derived ions within these regions difficult. The chemical noise originating from the matrix [29] is also at its highest level in these lower *m*/*z* regions.

In order to account for the changing levels of chemical noise over the *m*/*z* range of the spectrum, calculations for noise levels were undertaken for multiple regions throughout the acquired spectrum by measuring the standard deviation of the baseline. As with all subsequent spectra discussed in this article, ion assignments were only considered for reproducible peaks detected at or above an *S*/*N* threshold of 3:1. Detailed inspection of the spectrum

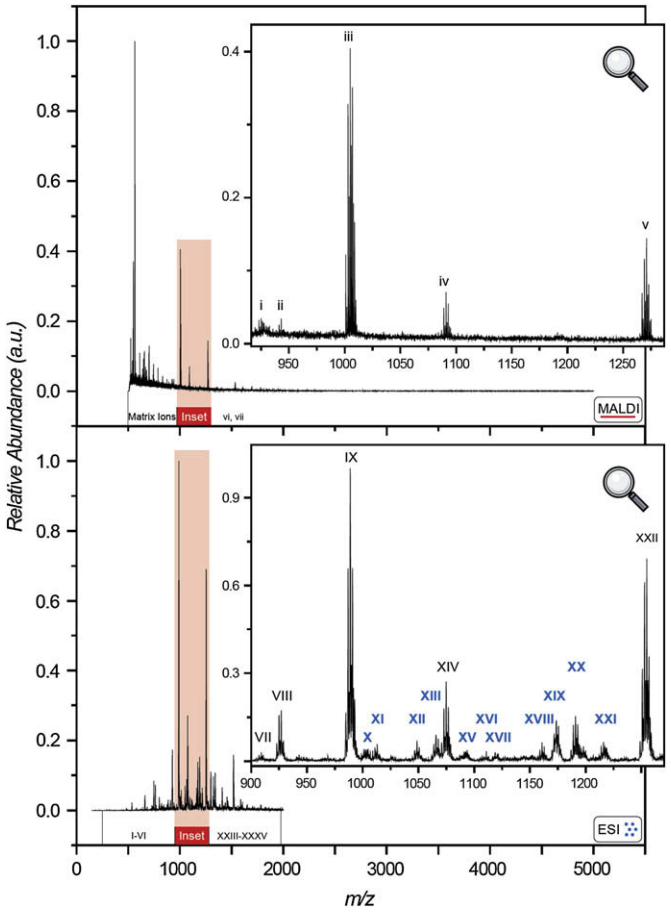

Fig. 1. Typical spectra from the ATRP initiator sample obtained via MALDI (above) and ESI (below) shown over a 0–5500 *m*/*z* range. The insets illustrate details of these spectra shown over the highlighted [48] *m*/*z* ranges. Peaks corresponding to ions only identified in ESI derived spectra are marked in blue. (For interpretation of the references to color in this figure legend, the reader is referred to the web version of this article).

reveals the presence of not only the 4-armed ATRP initiator as a potassium adduct (peak iii [49]), but also of 6 additional lower abundance ions. Peaks v–vii of Fig. 1 can be attributed to 5 and 6-armed side-products formed during the initiator synthesis, detected as potassium adducts (these products feature 5 or 6 Br end-group functionalities; see Scheme 4 for illustrated examples of these product assignments). The assignment of these products to peaks v–vii is supported by the comparison of the experimentally observed isotopic peak patterns with simulated peak patterns, indicating that peaks v/vi and vii do indeed arise from products containing 5 and 6 Br atoms respectively (see Fig. S2 of the Supplementary data for illustrations of these isotopic peak pattern comparisons). The isotopic peak patterns of peaks i and ii reveal the presence of only 3 Br atoms in these adduct species, initially suggesting that these peaks may by attributable to ions formed from in-source loss of Br end-groups from the 4, 5 or 6-armed products. However collisional activation in MS/MS product scans on these 4, 5 or 6-armed precursor ions via ESI (see Section 3.3.2, below) indicate that peaks i and ii arise from distinct side-products formed during the initiator synthesis. A summary of these ion assignments has been presented in Table S1, with the identified initiator side-products labelled as "SP#".

3.3.2. ESI-MS results

An inspection of the ESI derived data (lower portion of Fig. 1) reveals that noise levels remain relatively consistent across the m/z range of the acquired spectrum, and that all of the products identified via MALDI are also detected via ESI as sodium adducts. Some further improvement in the S/N of certain peaks was obtained by detecting the ions using the *ZoomScan* [50] mode of the LCQ Deca ion trap instrument. In addition to adducts formed from products that were also detected via MALDI, an additional 28 adducts are identified via ESI. In order to reveal whether or not these adducts arise due to in-source fragmentation, collisional activation in MS/MS product scans were conducted upon the precursor ions formed from the 4, 5 and 6-armed products already assigned to the spectrum (see Fig. S4 of the Supplementary data for an example of such an MS/MS spectrum). The MS/MS experiments revealed that the dominant in-source fragmentation pathways produce products in which terminal Br functionalities are removed via HBr elimination. As the additional adduct species observed in the ESI spectrum do not correspond to products formed via these fragmentation pathways, this would strongly suggest that these adducts arise as a result of distinct products within the sample under investigation, and not in-source fragmentation. Thus it can be concluded that when ESI is used instead of MALDI, 28 additional side-products can be identified in the initiator sample (a summary of the ion assignments for ESI derived spectra of the initiator sample is presented in Table 1 and S2).

A comparison of the ESI and MALDI derived mass spectra from the initiator sample reveals that for products identified via both ionisation protocols, the initiator side-product ions are detected in

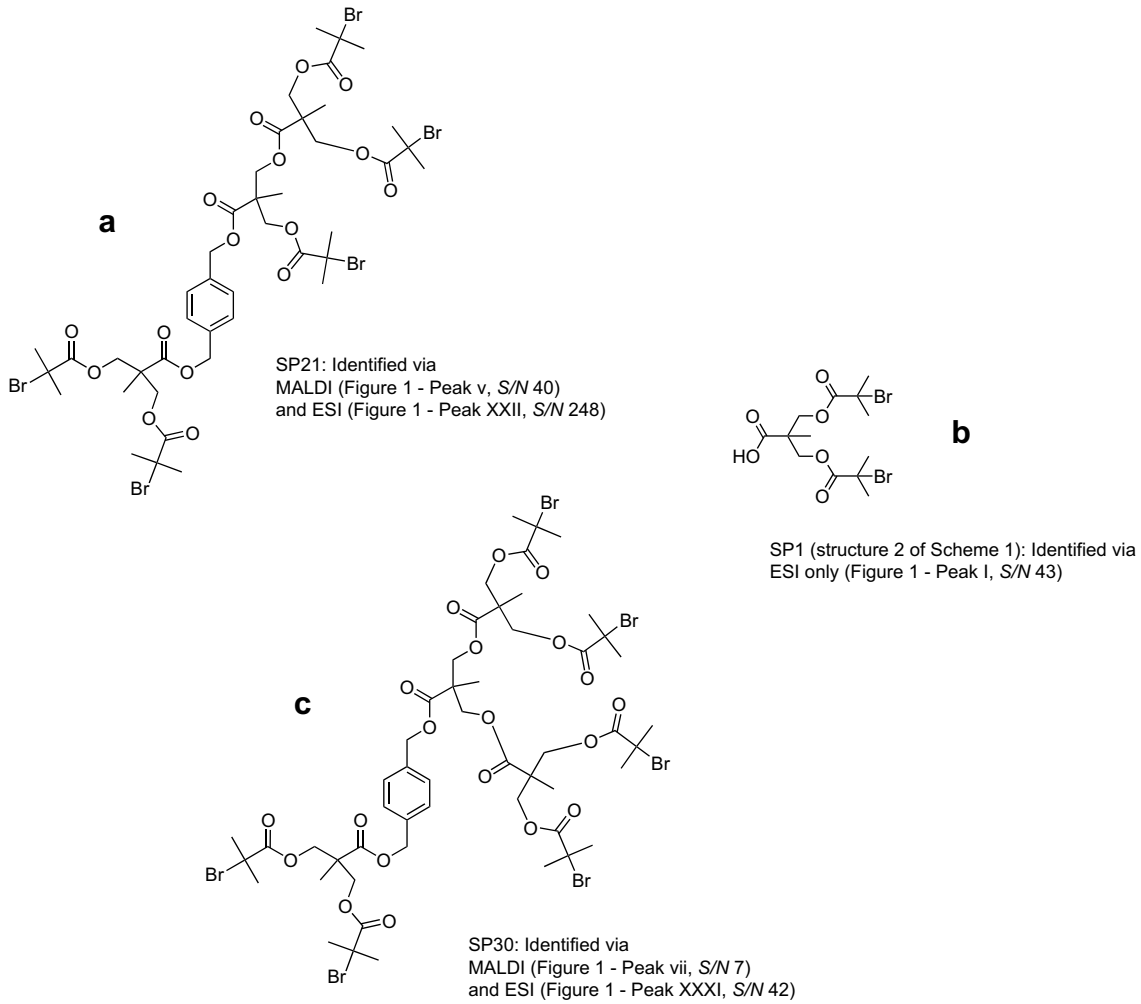

Scheme 4. Examples of initiator side-products identified in MALDI and/or ESI mass spectra: (a) 5-armed side-product, (b) precursor molecule, and (c) 6-armed side-product.

higher abundances relative to the 4-armed ATRP initiator ion in the ESI spectra. This suggests that the detection of more products via ESI relative to MALDI in the initiator sample can largely be attributed to a sample specific favourable ionisation of lower abundance species when using the employed ESI process, rather than more products being detected via ESI simply because of superior *S*/*N* levels (see Section 3.6 for further discussion).

3.4. Lower conversion poly(MA) star MS analysis

Following the MS analysis of the initiator sample, the previously described structural library was updated to incorporate polymer species associated with the identified initiator side-products. Using the updated structural library, an analysis of MALDI and ESI data obtained from a poly(MA) sample (theoretical DP_n after 100% conversion = 15 MA units/star arm; polymerisation ceased after 5 min) synthesised using the ATRP initiator analysed in the previous section is presented. The relatively low conversion poly(MA) sample is in contrast to the higher conversion poly(MA) sample, the analysis of which has been described in Section 3.5.

3.4.1. MALDI–MS results

The upper portion of Fig. 2 shows a typical mass spectrum obtained from the lower conversion poly(MA) sample via MALDI, shown over a 0–3000 *m*/*z* range. Details of this spectrum, the highlighted regions labelled as A and B, are presented in Fig. 3. As with the MALDI derived spectra obtained from the initiator sample, matrix ions dominate the lower *m*/*z* regions of the spectrum, and the levels of chemical noise increase as *m*/*z* decreases. To account for the changing levels of chemical noise, *S*/*N* calculations were conducted using noise levels estimated from multiple regions of the spectrum. In addition to the aforementioned reproducibility and *S*/*N* requirements in detecting ion signals, ion assignments were only considered for peaks which could be identified as arising from adducts formed from an oligomeric product; that is, for peaks repeating throughout the spectrum at *m*/*z* intervals corresponding to the exact mass of the methyl acrylate repeat unit divided by the charge state of the adduct (this criterion is also used in the assessment of ion signals in subsequent spectra described in this article).

A detailed inspection of the spectrum shown in Figs. 2 and 3 identifies the presence of 5 distinct oligomeric species within the sample. Potassium adducts formed from star polymers generated from the 4-armed ATRP initiator and featuring intact Br end-group functionalities (the Ideal Star illustrated in Scheme 2) are the dominant ions observed in the spectrum (peak iii of Fig. 3). In addition to these Ideal Stars, oligomeric chains generated from initiator side-products are also identified; specifically, potassium adducts formed from 2 and 5-armed initiator side-products which feature intact terminal Br functionalities (peaks i and iv of Fig. 3). Potassium adducts of two additional products are also identified (peaks ii and v of Fig. 3); although the origin of these oligomeric products remains unclear, collisional activation in MS/MS product scans on selected precursor ions conducted via ESI indicate that these ions result from distinct products within the sample, and not from in-source fragmentation (see Section 3.4.2 below for further elaboration). A summary of these ion assignments has been presented in Table 2, with the identified initiator side-product derived polymers labelled as "Poly-SP#" (examples of which are illustrated in Scheme 5).

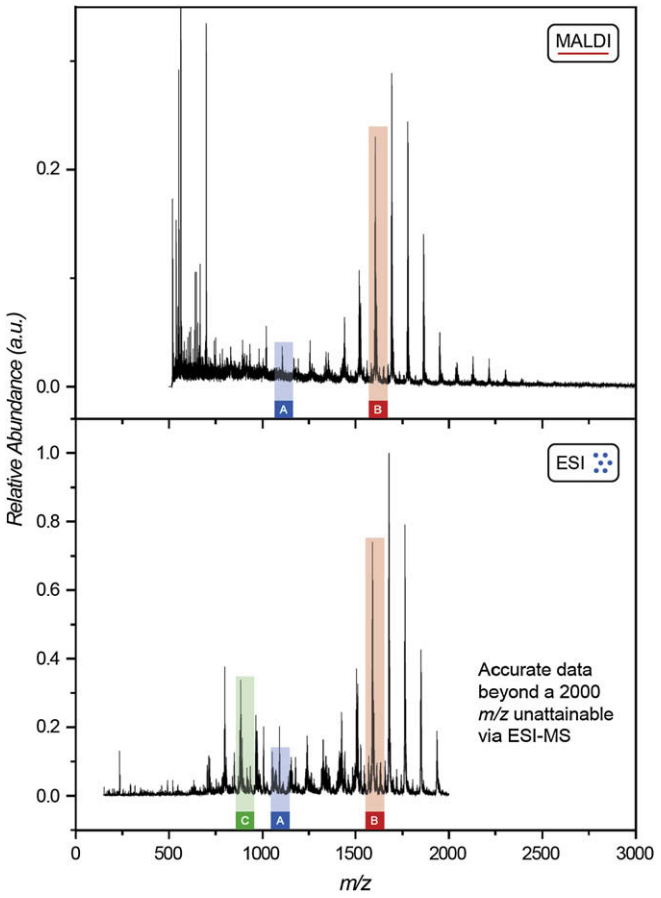

Fig. 2. Typical spectra from the lower conversion poly(MA) star sample obtained via MALDI (above) and ESI (below) shown over a 0–3000 *m*/*z* range. Details of these spectra are also presented over the smaller *m*/*z* ranges labelled A, B and C [48] (Fig. 3 and S5 respectively).

Table 1
A summary of the ion assignments for peaks identified in spectra obtained from the ATRP initiator sample via ESI, an example of which has been illustrated in Fig. 1. Illustrative *m*/*z* and maximum *S*/*N* have been shown for the respective ion signals.

Peak label	Ion assignment	*m*/*z* [51]	*S*/*N* [52,53]
I	$[SP1 + Na]^+$	454.9	21 (43)
II	$[SP2 + Na]^+$	536.0	28 (214)
III	$[SP3 + Na]^+$	661.0	12
VII	$[SP7 + Na]^+$	909.1	8
VIII	$[SP8 + Na]^+$	927.0	46
IX	$[Initiator + Na]^+$	988.9	266 (1006)
XIV	$[SP13 + Na]^+$	1074.9	72
XXII	$[SP21 + Na]^+$	1254.8	184 (248)
XXV	$[SP24 + Na]^+$	1340.8	29
XXXI	$[SP30 + Na]^+$	1518.7	42

Total number of distinct products within the sample identified via ESI = 35. (Only selected peak assignments are listed; a comprehensive list of peak assignments is presented in Table S2).

3.4.2. ESI-MS results

The lower portion of Fig. 2 shows a typical spectrum obtained from the lower conversion poly(MA) sample via ESI. Figs. 3 and S5 show typical spectra obtained using the *ZoomScan* mode of the LCQ Deca ion trap instrument employed in the ESI analysis for the *m*/*z* ranges labelled A, B and C in Fig. 2, respectively. For each of these spectra, the noise levels remain relatively consistent throughout their *m*/*z* ranges.

A close inspection of the spectra identifies the presence of 11 distinct adduct species. When considering the full available *m*/*z* range of the LCQ Deca ion trap instrument, the most dominant adduct species observed from the sample can be attributed to sodium adducts formed from Ideal Stars and Poly-SP2 (peak VI of Fig. 3, and peak I of Fig. S5, respectively). 3 additional initiator

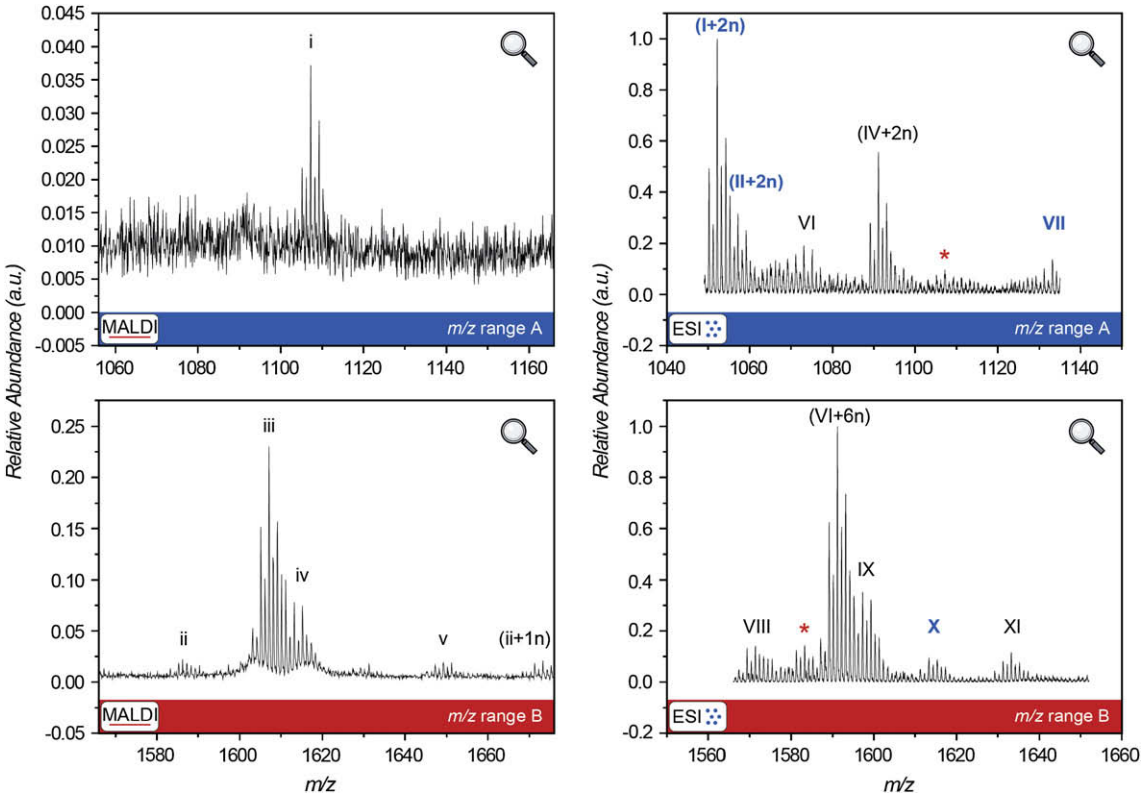

Fig. 3. Details of a typical spectrum from the lower conversion poly(MA) star sample obtained via MALDI (left), and typical spectra from the same sample obtained via ESI using the *ZoomScan* mode (right). Spectra are shown over the *m*/*z* ranges A and B of Fig. 2 [48]. Peaks corresponding to oligomeric adducts only identified in ESI derived spectra are marked in blue, and non-reproducible peaks at an *S*/*N* above 3:1 are marked with a red asterisk. (For interpretation of the references to color in this figure legend, the reader is referred to the web version of this article.)

side-product derived oligomers are also identified: Poly-SP1, Poly-SP3 and Poly-SP21 (peaks II and IV of Fig. 3 and S5, and peak IX of Fig. 3, respectively; see Scheme 5 for illustrations of Poly-SP1 and Poly-SP21). An additional adduct which produces peak III of Fig. S5 can be attributed to doubly charged Ideal Stars, and the chemical structures of the remaining adducts observed in the spectra are not immediately identifiable from the structural library (peaks V, VII, VIII, X and XI). Again, collisional activation in MS/MS product scans was conducted upon precursor ions to which chemical structures were confidently assigned. These experiments produced a wide range of product ions, none of which correspond to the adducts observed in the spectra shown in Figs. 2 and 3 and S5. It can therefore be concluded that the adducts which give rise to peaks V, VII, VIII, X and XI are due to distinct oligomeric species within the polymer sample, and not to in-source fragmentation.

All of the products identified via MALDI are also detected via ESI as sodium adducts, and since all of the ions identified in the ESI spectra can be attributed to distinct products within the sample (with the exception of the doubly charged peak III), it can be concluded that 5 additional products are detected in the sample when using ESI rather than MALDI. A summary of the ion assignments for the ESI derived spectra of the lower conversion poly(MA) sample is presented in Table 3.

Table 2
A summary of the ion assignments for peaks identified in spectra obtained from the lower conversion poly(MA) star sample via MALDI, an example of which has been illustrated in Figs. 2 and 3. Illustrative *m*/*z* and maximum *S*/*N* have been shown for the respective ion signals.

Peak label	Ion assignment	*m*/*z* [51]	DP_n [54]	*S*/*N* [52]
i	$[Poly\text{-}SP3 + K]^+$	1107.2	3–7	5
ii	$[Poly\text{-}3 + K]^+$	1587.3	$n-(n+3)$	6
iii	$[Ideal\ Star + K]^+$	1607.1	5–13	83
iv	$[Poly\text{-}SP21 + K]^+$	1613.2	1–13	8
v	$[Poly\text{-}5 + K]^+$	1649.2	$n-(n+4)$	7

Total number of distinct products within the sample identified via MALDI = 5.

3.5. Higher conversion poly(MA) star MS analysis

An analysis of MALDI and ESI data obtained from a poly(MA) sample (theoretical DP_n after 100% conversion = 6 MA units/star arm; polymerisation ceased after 40 min) synthesised using the previously analysed ATRP initiator is presented below; this relatively high conversion sample is in contrast to the lower conversion sample analysed in Section 3.4.

3.5.1. MALDI–MS results

The upper portion of Fig. 4 shows a typical mass spectrum obtained from the higher conversion poly(MA) sample via MALDI, shown over a 0–4000 *m*/*z* range. Details of this spectrum, the highlighted regions labelled as A and B, are presented in Figs. 5 and S6 respectively. As with the previously discussed MALDI derived spectra, matrix ions dominate the lower *m*/*z* regions of the spectrum and the levels of chemical noise are at a maximum at relatively low *m*/*z* ranges. *S*/*N* calculations were conducted using the same protocol as outlined in previous MALDI results sections.

One of the most apparent features of spectra obtained from the higher conversion poly(MA) sample is that all of the detected ions contain no Br atoms. This was ascertained from the experimentally observed isotopic peak patterns, which do not display the distinct characteristics of Br-containing species (for example, see Fig. S3 of the Supplementary data). It is thus apparent that terminal Br loss

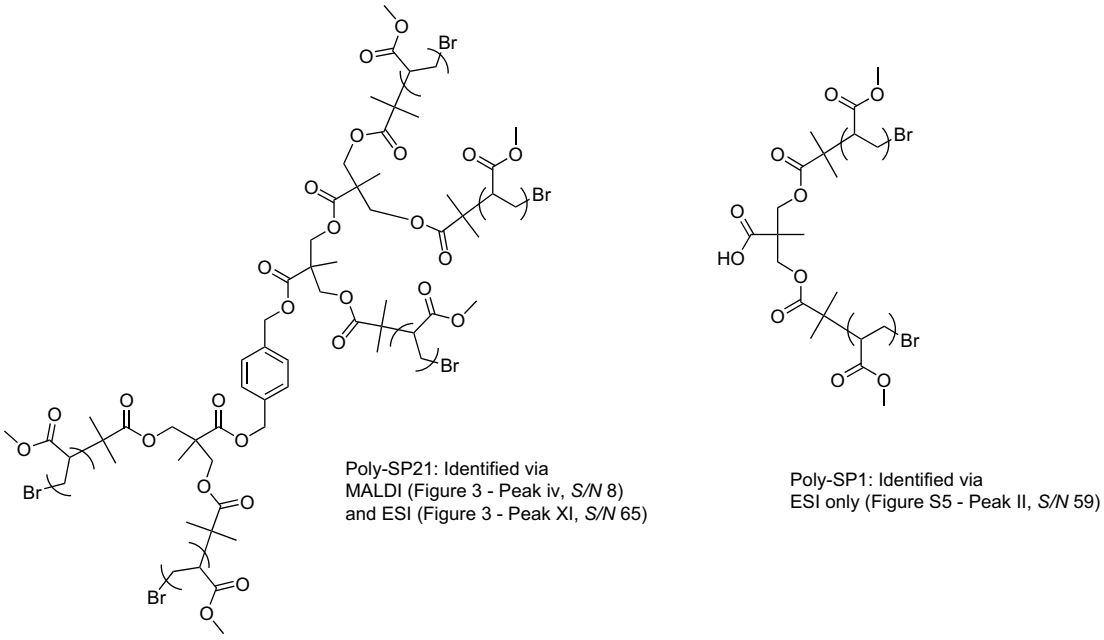

Scheme 5. Examples of initiator side-product derived oligomers identified in MALDI and/or ESI mass spectra of the lower conversion poly(MA) sample.

has occurred in any initiator or initiator side-product derived oligomers observed in the spectra. In the naming of these products throughout the remainder of this article, products in which Br end-group loss has occurred have been labelled according to the end-group functionalities replacing the terminal Br atoms. For example, Ideal Stars featuring 4 proton end-groups are labelled "Ideal Star(4H)", and Ideal Stars featuring 2 proton end-groups and 2 "Ac1" end-groups (as discussed below) are labelled "Ideal Star(2H,2Ac1)".

A closer inspection of the spectrum shown in Figs. 4 and 5 and S6 reveals that the 4-armed star products and side-product derived oligomeric chains observed in the lower conversion poly(MA) sample are now predominantly detected as products in which all of the terminal Br functionalities have been replaced with protons (peaks iii–v of Fig. 5, and peaks vii and xvi of Fig. S6; see Scheme 7 for an illustration of the Ideal Star(4H) product). These proton end-group containing species are detected as potassium adducts, and also occasionally as lower abundance sodium adducts. As the higher conversion poly(MA) sample was analysed with identical MALDI ionisation conditions as the lower conversion poly(MA) sample in which intact oligomeric chains were observed, it is

Table 3
A summary of the ion assignments for peaks identified in spectra obtained from the lower conversion poly(MA) star sample via ESI, examples of which have been illustrated in Figs. 2 and 3 and S5. Illustrative *m/z* and maximum *S/N* have been shown for the respective ion signals.

Peak label	Ion assignment	*m/z* [51]	DP_n [54]	*S/N* [52,55]
I	$[Poly\text{-}SP2 + Na]^+$	880.2	1–7	47 (59)
II	$[Poly\text{-}SP1 + Na]^+$	885.1	1–7	17 (31)
III	$[Ideal\ Star + Na_2]^{2+}$	893.2	6–14	34 (33)
IV	$[Poly\text{-}SP3 + Na]^+$	919.2	2–9	40 (30)
V	$[Poly\text{-}1 + M]^+$	925.3	n–$(n+4)$	20 (10)
VI	$[Ideal\ Star + Na]^+$	1073.2	1–11	198 (101)
VII	$[Poly\text{-}2 + M]^+$	1133.1	n–$(n+5)$	6 (7)
VIII	$[Poly\text{-}3 + Na]^+$	1571.4	n–$(n+5)$	20 (14)
IX	$[Poly\text{-}SP21 + Na]^+$	1597.3	1–5	65 (36)
X	$[Poly\text{-}4 + M]^+$	1613.3	n–$(n+5)$	30 (9)
XI	$[Poly\text{-}5 + Na]^+$	1633.3	n–$(n+5)$	19 (11)

Total number of distinct products within the sample identified via ESI = 10.

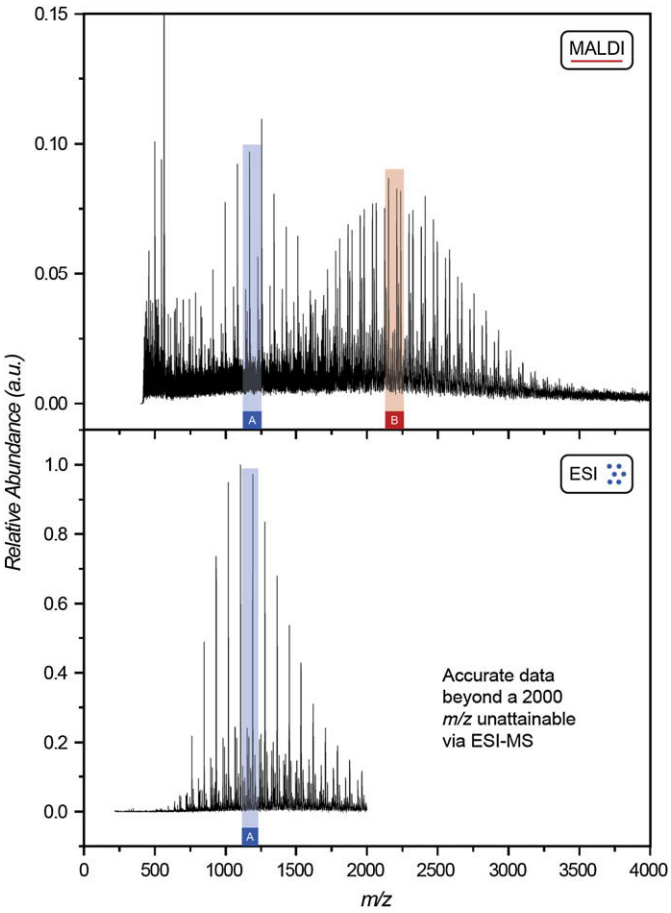

Fig. 4. Typical spectra from the higher conversion poly(MA) star sample obtained via MALDI (above) and ESI (below) shown over a 0–4000 *m/z* range. Details of these spectra are also presented over the smaller *m/z* ranges labelled A and B [48] (Fig. 5 and S6 respectively).

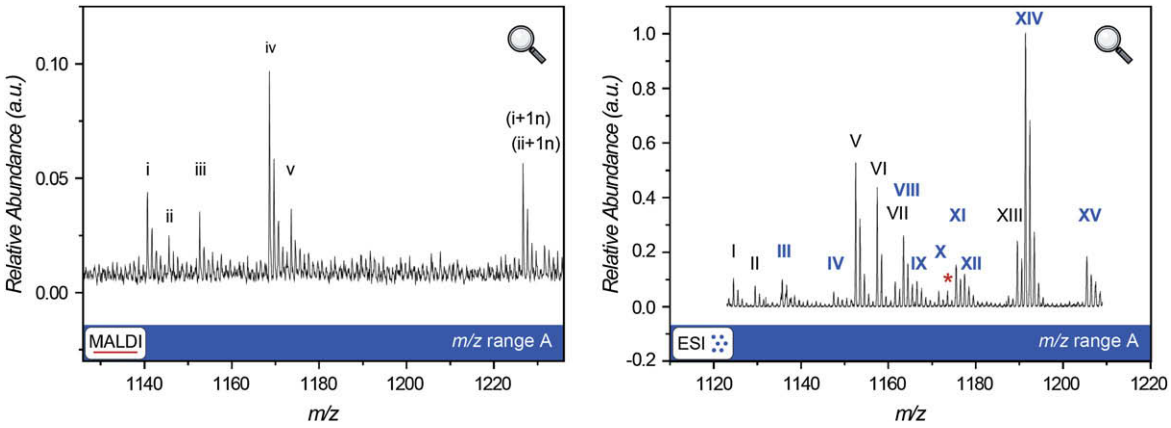

Fig. 5. Detail of a typical spectrum from the higher conversion poly(MA) star sample obtained via MALDI (left), and a typical spectrum from the same sample obtained via ESI using the *ZoomScan* mode (right). Spectra are shown over the *m*/*z* range A of Fig. 4 [48]. Peaks corresponding to oligomeric adducts only identified in ESI derived spectra are marked in blue, and non-reproducible peaks at an *S*/*N* above 3:1 are marked with a red asterisk. (For interpretation of the references to color in this figure legend, the reader is referred to the web version of this article.)

unlikely that terminal Br loss has occurred via in-source fragmentation. Moreover, since no products containing terminal unsaturation are observed, as would be expected if termination via disproportionation was occurring, these proton end-group containing species cannot be explained by disproportionation reactions. Rather, it would appear that these products are forming via the known phenomenon of degradative transfer at high conversions via hydrogen radical extraction when polymerising acrylate monomers [17,45]. This phenomenon is known to occur when an excess of PMDETA relative to the initiator is used in the ATRP polymerisations, with the ligand PMDETA most probably acting as the hydrogen donor. Such reaction conditions, earlier identified as being necessary for the formation of star polymers [56], are indeed consistent with the polymer sample under investigation (see Section 2.4).

In addition to the products in which terminal Br loss has occurred via proton replacement, 8 additional ions are detected in the MALDI spectrum. None of these ions are immediately identifiable via the structural library. Collisional activation in MS/MS product scans conducted by ESI on the proton end-group containing precursor ions indicate that these additional ions are not formed due to in-source fragmentation, as they do not match up with the observed product ion peaks. Furthermore it is notable that many of these ions are detected at *m*/*z* intervals of 58 and/or 56 units higher than the proton end-group containing adducts. In considering the origin of these ions it should be noted that acetone, the solvent used in the synthesis of the polymer sample, is known to produce the radical $(CH_3)_2\dot{C}OH$ in the presence of a hydrogen donor, with the formation of the radicals $\dot{C}H_3$ and $\dot{C}H_2COCH_3$ also being likely [57,58]. Thus, with PMDETA acting as a hydrogen donor in the polymerisation in question, the formation of such radical species during the polymerisation is probable. The reaction of acetone with any methyl radicals that are generated provides an additional avenue by which the radical $\dot{C}H_2COCH_3$ can be formed [59,60]. A summary of these reactions has been provided in Scheme 6, with the acetone derived radicals $(CH_3)_2\dot{C}OH$, $\dot{C}H_3$ and $\dot{C}H_2COCH_3$ referred to as Ac1, Ac2 and Ac3 respectively. Products formed via degradative transfer reactions on one or more star arms involving the radicals Ac1 and Ac3, in a similar manner to the hypothesised degradative transfer reactions involving hydrogen radicals donated by PMDETA, can serve to explain all of the ions detected at *m*/*z* intervals of 58 and/or 56 units higher than the adducts formed from solely proton end-group containing species. These Ac1 and Ac3 derived products are detected as potassium adducts (peaks i and ii of Fig. 5, and peaks x–xii, xiv and xv of Fig. S6) and also occasionally as lower abundance sodium adducts (peak iii of Fig. 5, and peaks viii and xiii of Fig. S6). Examples of these products are illustrated in Scheme 7.

In total, 12 distinct products are identified in the higher conversion poly(MA) sample via MALDI, and a summary of the MALDI derived ion assignments for this sample has been presented in Table 4.

3.5.2. ESI-MS results

The lower portion of Fig. 4 shows a typical spectrum obtained from the higher conversion poly(MA) sample via ESI, and Fig. 5 shows a typical spectrum obtained using the *ZoomScan* mode of the LCQ Deca ion trap instrument employed in the ESI analysis over the *m*/*z* range labelled A in Fig. 4. For each of these spectra, the noise levels remain relatively consistent throughout their *m*/*z* ranges.

It was apparent in the MALDI spectra of the higher conversion poly(MA) sample that products could be identified in *m*/*z* regions well above 2000; however, the 2000 *m*/*z* limit for obtaining

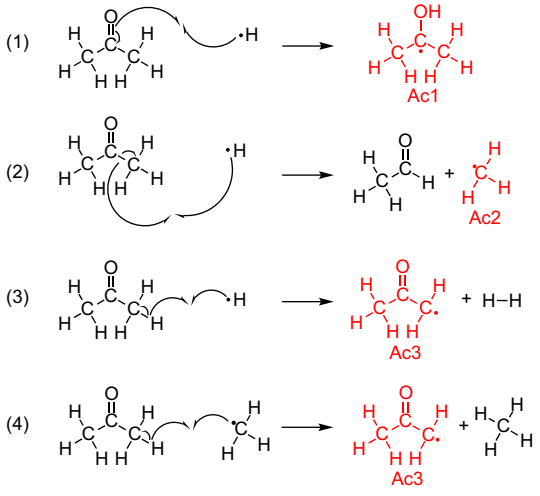

Scheme 6. A summary of likely radical reactions involving acetone in ATRP mediated polymerisations featuring PMDETA as the ligand and acetone as a solvent. MS data supports the hypothesis that the acetone derived radicals marked in red (labelled as Ac1, Ac2 and Ac3) can replace terminal Br functionalities in the poly(MA) system under investigation.

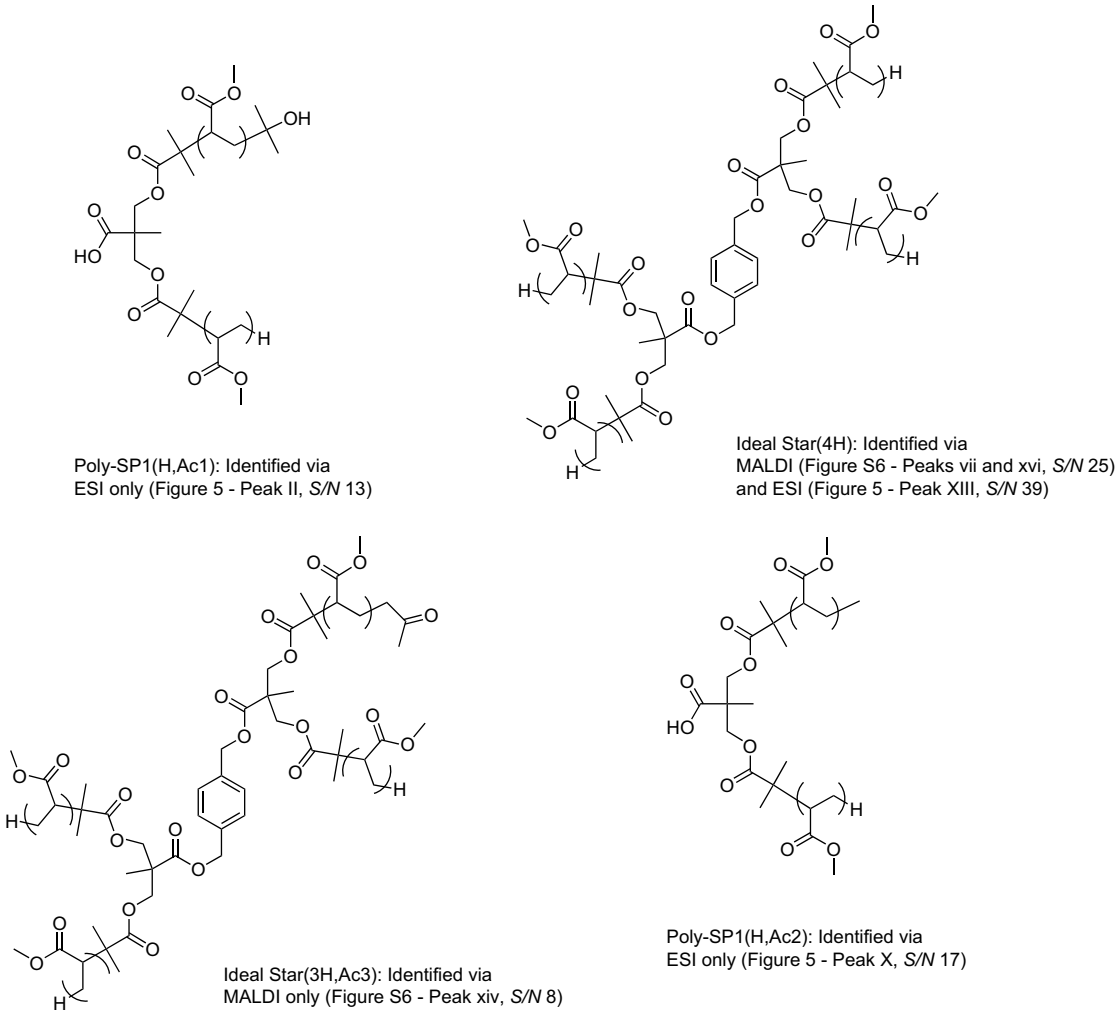

Scheme 7. Examples of oligomers identified in MALDI and/or ESI mass spectra of the higher conversion poly(MA) sample in which elimination of terminal Br functionalities has occurred.

accurate data from the LCQ Deca ion trap instrument employed in the present study limits the number of ions able to be detected using this ESI instrument. Despite this severe disadvantage, 15 distinct products are detected in the higher conversion poly(MA) sample using ESI, as opposed to 12 when using MALDI. The ESI spectra shown in Figs. 4 and 5 are dominated by initiator side-product derived oligomer chains in which the terminal Br functionalities are replaced with protons; that is, the products Poly-SP2(2H), Poly-SP1(2H) and Poly-SP3(2H) (peaks V, VI and XIV of Fig. 5, respectively). Further to this, the tail end of the Ideal Star(4H) distribution observed in the MALDI spectra is also detected via ESI (peak XIII of Fig. 5). All of these products are observed as sodium adducts. MS/MS experiments conducted upon these adducts produced no product ions that corresponded to any of the ions observed in the spectra shown in Figs. 4 and 5, indicating that all of the ions observed in these spectra arise due to distinct products within the sample.

Table 4
A summary of the ion assignments for peaks identified in spectra obtained from the higher conversion poly(MA) star sample via MALDI, an example of which has been illustrated in Figs. 4 and 5 and S6. Illustrative m/z and maximum S/N have been shown for the respective ion signals.

Peak label	Ion assignment	m/z	DP_n [54]	S/N [52]
i	$[Poly\text{-}SP2(H,Ac1)+K]^+$	1140.7	4–15	6
ii	$[Poly\text{-}SP1(H,Ac1)+K]^+$	1145.6	7–11	3
iii	$[Poly\text{-}SP2(2H)+Na]^+$	1152.6	6–12	4
iv	$[Poly\text{-}SP2(2H)+K]^+$	1168.6	4–18	13
v	$[Poly\text{-}SP1(2H)+K]^+$	1173.6	6–26	4
vi	$[Poly\text{-}6+M]^+$	2150.1	$n-(n+11)$	7
vii	$[Ideal\ Star(4H)+K]^+$	2152.0	7–31	25
viii	$[Ideal\ Star(2H,2Ac1)+Na]^+$	2166.1	14–20	5
ix	$[Poly\text{-}7+M]^+$	2168.2	$n-(n+25)$	6
x	$[Ideal\ Star(2H,2Ac3)+K]^+$	2178.1	14–20	4
xi	$[Ideal\ Star(2H,Ac1,Ac3)+K]^+$	2180.1	10–26	6
xii	$[Ideal\ Star(2H,2Ac1)+K]^+$	2182.1	10–29	8
xiii	$[Ideal\ Star(3H,Ac1)+Na]^+$	2194.1	10–29	8
xiv	$[Ideal\ Star(3H,Ac3)+K]^+$	2208.0	9–23	8
xv	$[Ideal\ Star(3H,Ac1)+K]^+$	2210.2	7–31	24
xvi	$[Ideal\ Star(4H)+Na]^+$	2222.2	7–31	13

Total number of distinct products within the sample identified via MALDI = 12.

In a similar manner to the MALDI spectra, ions are detected at m/z intervals of 58 units higher than the adducts formed from solely proton end-group containing products and thus can be attributed to Ac1 derived products (peaks I–IV, VII and VIII of Fig. 5). Additionally, ions detected at m/z intervals of 14 units higher can be attributed to Ac2 derived products (peaks IX, X, XII and XV of Fig. 5), lending further evidence to support the hypothesis that the acetone derived radicals can replace terminal Br functionalities in the poly(MA) system under investigation. Examples of these products in which elimination of terminal Br functionalities has occurred are shown in Scheme 7. Interestingly, no Ac3 derived products are observed in the ESI spectra despite

these products being detected at significant abundances in the MALDI spectra, while no Ac2 derived products were observed in the MALDI spectra. This suggests that sample specific chemical ionisation bias effects have an impact on the ability for each ionisation method to detect these specific products within the given sample (this is discussed further in Section 3.6). A summary of the ESI derived ion assignments for the higher conversion poly(MA) sample has been presented in Table 5.

3.6. Comparative performance of MALDI and ESI

Having analysed the initiator and polymer samples using MALDI and ESI, the following section discusses the comparative performances of the specific ionisation protocols used in identifying the products within these samples, and the relative merits of each technique to allow mechanistic insights to be gained into the polymerisations under investigation. How these specific results relate to the broader question of the general comparability of MALDI and ESI in the analysis of synthetic polymers is also discussed.

Fig. 6 compares the total number of unique and shared products identified in the three samples via the two ionisation protocols employed in the study (Fig. S8 shows similar information for each individual sample). It can be seen that ESI allows a significantly greater number of products to be identified when compared to MALDI; this is a consistent occurrence across all three samples, even in the higher conversion poly(MA) sample in which products were identified via MALDI at m/z regions higher than those accessible to the employed ESI instrument. The superior ability of ESI over MALDI to comprehensively detect the distinct chemical species present in these samples can be attributed to several factors: (a) lower noise levels in the spectra acquired via ESI, (b) matrix ion interference at lower m/z regions in the spectra acquired via MALDI and (c) sample specific favourable ionisation of certain products when using ESI. The discussion below focuses upon how these factors relate to the conditions of the present study, and the applicability of these factors when considering the general comparability of MALDI and ESI in the analysis of synthetic polymers.

With regard to factor (a), it was observed that the S/N′s for ions detected via ESI are consistently superior to those observed via MALDI (see Fig. S7 of the Supplementary data), the one exception being adducts formed from the Ideal Star(4H) product observed in the higher conversion poly(MA) sample of which only

Table 5
A summary of the ion assignments for peaks identified in spectra obtained from the higher conversion poly(MA) star sample via ESI, examples of which have been illustrated in Figs. 4 and 5. Illustrative m/z and maximum S/N have been shown for the respective ion signals.

Peak label	Ion assignment	m/z	DP_n [54]	S/N [52,55]
I	$[Poly\text{-}SP2(H,Ac1)+Na]^+$	1124.5	5–13	22 (17)
II	$[Poly\text{-}SP1(H,Ac1)+Na]^+$	1129.5	8–14	11 (13)
III	$[Poly\text{-}SP3(2Ac1)+Na]^+$	1135.7	4–16	24 (17)
IV	$[Poly\text{-}9(Ac1)+M]^+$	1147.5	$n-(n+11)$	12 (8)
V	$[Poly\text{-}SP2(2H)+Na]^+$	1152.6	2–18	60 (88)
VI	$[Poly\text{-}SP1(2H)+Na]^+$	1157.5	5–15	50 (73)
VII	$[Ideal\ Star(3H,Ac1)+Na]^+$	1161.5	2–14	16 (15)
VIII	$[Poly\text{-}SP3(H,Ac1)+Na]^+$	1163.4	1–15	54 (44)
IX	$[Poly\text{-}SP2(H,Ac2)+Na]^+$	1166.5	7–17	17 (15)
X	$[Poly\text{-}SP1(H,Ac2)+Na]^+$	1171.5	10–13	17 (8)
XI	$[Poly\text{-}9+M]^+$	1175.5	$n-(n+16)$	31 (26)
XII	$[Poly\text{-}SP3(Ac1,Ac2)+Na]^+$	1177.4	1–16	29 (20)
XIII	$[Ideal\ Star(4H)+Na]^+$	1189.5	4–15	33 (39)
XIV	$[Poly\text{-}SP3(2H)+Na]^+$	1191.4	2–17	251 (166)
XV	$[Poly\text{-}SP3(H,Ac2)+Na]^+$	1205.4	5–17	33 (31)

Total number of distinct products within the sample identified via ESI = 15.

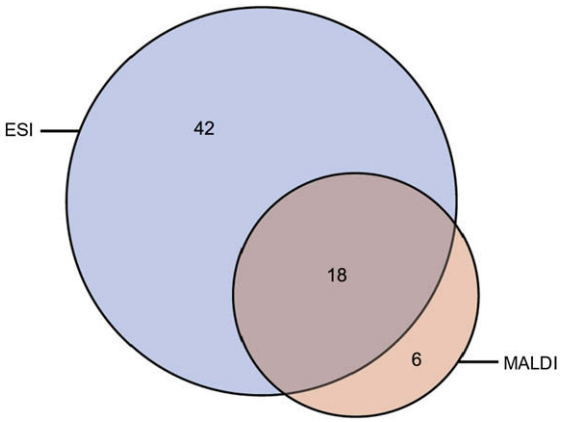

Fig. 6. Venn diagram showing the number of unique and shared products identified via the MALDI and ESI protocols employed in the present study for the three samples under investigation.

the tail end of the product distribution was able to be detected via ESI. In this present investigation, the higher quality S/N′s observed in the ESI spectra were likely to have played a role in this ionisation technique's ability to detect a greater number of products when compared to MALDI. In considering factor (b), when compared to the ESI spectra, certain lower m/z ions observed in the MALDI spectra were detected at low relative abundances; it is feasible that detector saturation from intense matrix peaks could have reduced the detection efficiency of these ions. Furthermore it was a general feature of all of the MALDI derived spectra that the detection of sample derived ions below a given m/z range was difficult or impossible due to the presence of abundant matrix ions. When considering the contribution of these factors towards the superior performance of ESI over the employed MALDI technique, it is important to note that the matrix, solvent, salt and sample preparation in any MALDI experiment should ideally result in homogeneous matrix and sample co-crystallisation, and that the traditional dried droplet method used in this study was unlikely to be the optimal means of achieving this. Inconsistent shot-to-shot signal reproducibility coming as a result of inhomogeneous co-crystallisations was likely to have contributed towards chemical noise and matrix ion interference. Though it is difficult to generalise that ESI will produce spectra featuring higher S/N′s than MALDI across different sample preparation methods, polymer classes and MS instrumentation, and though it is likely that improvements in the observed levels of chemical noise, decreases in matrix ion interference and improved detection limits [61] could have been achieved through more advanced MALDI sample preparation methods than the dried droplet technique, it is noteworthy that the issues of matrix derived chemical noise and ion interference are bypassed completely when using ESI.

Factor (c), the sample specific favourable ionisation of certain products when using ESI, was apparent for products in all 3 of the samples under study. Although MALDI also showed an ability to more effectively ionise certain products in the higher conversion poly(MA) sample when compared to ESI, in general, ESI showed a greater tendency towards the effective ionisation of lower abundance products than MALDI. Given the fact that the two ionisation protocols under study are completely distinct, there are numerous factors that can contribute towards such a difference in ionisation tendencies. For example, a fractionation of polymer samples during the matrix and sample co-crystallisation phase in MALDI sample preparation due to the presence of molecular weight, end-group functionality and/or structural distributions will

likely produce differing propensities towards ionisation for distinct chemical products. Though it is difficult to pinpoint the precise factors contributing towards the differing ionisation efficiencies, it is notable that the tendency towards more effective ionisation of lower abundance products observed in ESI over MALDI in the present study is echoed in the results described by Ladaviére et al. for poly(styrene) samples [16]. Additionally, the fact that the present results were not affected by in-source fragmentation complicating the observation of lower abundance ions through a limitation of the applicable MALDI laser intensity, as reported by Ladaviére et al. in their study, point towards a more general tendency towards the effective ionisation of lower abundance products via ESI when compared to MALDI.

4. Conclusions

By identifying the products present in a multifunctional ATRP initiator sample and poly(MA) samples synthesised using this initiator, comparative performances of ESI and MALDI ionisation protocols were able to be ascertained. The MS mechanistic studies conducted upon the system in question found that in addition to the main 4-armed product identified within the initiator sample, additional side-products were also present. Using this ATRP initiator, 4-armed poly(MA) stars were successfully synthesised, along with several side-products derived oligomers. At a relatively high monomer to polymer conversion, terminal Br loss was observed in the synthesised oligomers. This Br loss was hypothesised to occur via degradative transfer reactions involving hydrogen radicals donated by the ligand PMDETA, and the acetone derived radicals $(CH_3)_2\dot{C}OH$, $\dot{C}H_3$ and $\dot{C}H_2COCH_3$.

In performing these mechanistic investigations, ESI was found to be more effective in obtaining a comprehensive list of the distinct products present in the samples under investigation when compared to the employed MALDI technique. This was attributed to (a) lower noise levels in the spectra acquired via ESI, (b) matrix ion interference at lower m/z regions in the spectra acquired via MALDI and (c) sample specific favourable ionisation of certain products when using ESI. Though generalisations across all polymer classes and MS instrumentation are difficult to make, it was noted that issues of matrix derived chemical noise and ion interference are bypassed completely when using ESI, and that trends towards more effective ionisation of lower abundance products in ESI over MALDI are observed. This suggests that the utilisation of ESI must be strongly considered if the maximum number of end-group functionalities within a given polymer sample are to be identified via MS in a given polymer mechanistic investigation.

Acknowledgements

C.B.-K. acknowledges financial support from the *Karlsruhe Institute of Technology* (KIT) in the context of the *Excellence Initiative* for leading German universities as well as the *German Research Council* (DFG) and the *Ministry of Arts and Science* of the State of Baden-Württemberg. G.H.-S. acknowledges financial support from the *Australian Postgraduate Award* (APA). F.D.P. acknowledges the FWO and the *Belgian Program on Interuniversity Attraction Poles* initiated by the Belgian State, Prime Minister's office (Program P6/27) for financial support. M.L. is supported by a PhD grant of the Institute for the *Promotion of Innovation through Science and Technology in Flanders* (IWT-Vlaanderen). The authors gratefully acknowledge Dr. Arun Prasath Ramaswamy for assistance in producing the MALDI spectra; and Mr. Lewis Adler for helpful discussions and assistance in the editing of this article.

Appendix. Supplementary data

^{1}H NMR data obtained from the initiator sample; simulated and experimentally observed isotopic peak patterns for selected adduct ions; MS/MS spectrum from the 4-armed ATRP initiator; comprehensive tables of peak assignments for the initiator sample; additional spectra from the lower and higher conversion poly(MA) samples; comparison of maximum S/N readings for ions observed via both MALDI and ESI; and Venn diagrams showing the number of unique and shared products identified via MALDI and ESI for the individual samples under investigation. Supplementary data associated with this article can be found in the online version, at doi:10.1016/j.polymer.2009.03.009.

References

[1] Rader HJ, Schrepp W. Acta Polymerica 1998;49:272–93.
[2] Nielsen MWF. Mass Spectrometry Reviews 1999;18:309–44.
[3] Gruendling T, Guilhaus M, Barner-Kowollik C. Analytical Chemistry 2008;80:6915–27.
[4] Barner-Kowollik C, Davis TP, Stenzel MH. Polymer 2004;45:7791–805.
[5] Weidner SM, Trimpin S. Analytical Chemistry 2008;80:4349–61.
[6] Belu AM, DeSimone JM, Linton RW, Lange GW, Friedman RM. Journal of the American Society for Mass Spectrometry 1996;7:11–24.
[7] Hanton SD. Chemical Reviews 2001;101:527–69.
[8] Aksenov AA, Bier ME. Journal of the American Society for Mass Spectrometry 2008;19:219–30.
[9] For instance, without recourse to secondary means of ion identification such as tandem mass spectrometry, the assignment of certain peaks in a given mass spectrum may be considered virtually impossible if these peaks consist of overlapping signals due to the presence of multiply charged ions, and if the instrument's mass resolving power is insufficient to allow for differentiation of these signals.
[10] Barton Z, Kemp TJ, Buzy A, Jennings KR. Polymer 1995;36:4927–33.
[11] Guittard J, Tessier M, Blais JC, Bolbach G, Rozes L, Marechal E, et al. Journal of Mass Spectrometry 1996;31:1409–21.
[12] Latourte L, Blais JC, Tabet JC. Analytical Chemistry 1997;69:2742–50.
[13] Parees DM, Hanton SD, Cornelio Clark PA, Willcox DA. Journal of the American Society for Mass Spectrometry 1998;9:282–91.
[14] Hunt SM, Sheil MM. European Mass Spectrometry 1998;4:475–86.
[15] Alhazmi AM, Giguere MS, Dube MA, Mayer PM. European Journal of Mass Spectrometry 2006;12:301–10.
[16] Ladavière C, Lacroix-Desmazes P, Delolme F. Macromolecules 2009;42:70–84.
[17] Bednarek M, Biedron T, Kubisa P. Macromolecular Chemistry and Physics 2000;201:58–66.
[18] Hua DB, Ge XP, Tang J, Zhu ML, Bai RK. European Polymer Journal 2007;43:847–54.
[19] Nonaka H, Ouchi M, Kamigaito M, Sawamoto M. Macromolecules 2001;34:2083–8.
[20] Szablan Z, Junkers T, Koo SPS, Lovestead TM, Davis TP, Stenzel MH, et al. Macromolecules 2007;40:6820–33.
[21] Lovestead TM, Hart-Smith G, Davis TP, Stenzel MH, Barner-Kowollik C. Macromolecules 2007;40:4142–53.
[22] Hart-Smith G, Chaffey-Millar H, Barner-Kowollik C. Macromolecules 2008;41:3023–41.
[23] Ah Toy A, Vana P, Davis TP, Barner-Kowollik C. Macromolecules 2004;37:744–51.
[24] Feldermann A, Ah Toy A, Davis TP, Stenzel MH, Barner-Kowollik C. Polymer 2005;46:8448–57.
[25] Chaffey-Millar H, Hart-Smith G, Barner-Kowollik C. Journal of Polymer Science Part A Polymer Chemistry 2007;46:1873–92.
[26] No discernible improvements in S/N were obtained by signal averaging additional data.
[27] Karas M, Hillenkamp F. Analytical Chemistry 1998;60:2299–301.
[28] Silnikov EE, Sysoev AA, Sysoev AA, Fatyushina EV. Instruments and Experimental Techniques 2008;51:574–82.
[29] Krutchinsky AN, Chait BT. Journal of the American Society for Mass Spectrometry 2002;13:129–34.
[30] Hanton SD, Owens KG. Investigation of polymer and matrix solubility by MALDI and MESIMS. In: 46th ASMS Conference on Mass Spectrometry and Allied Topics. Orlando, FL; 1998. p. 1185.
[31] Meier MAR, Adams N, Schubert US. Analytical Chemistry 2007;79:863–9.
[32] Weinberger SR, Boernsen KO, Finchy JW, Robertson V, Musselman BD. An evaluation of crystallization methods for matrix-assisted laser desorption/ionization of proteins. In: 41st ASMS Conference of Mass Spectrometry and Allied Topics. San Francisco, CA; 1993. p. 775.
[33] Nicola AJ, Gusev AI, Proctor A, Jackson EK, Hercules DM. Rapid Communications in Mass Spectrometry 1995;9:1164–71.
[34] Gusev AI, Wilkinson WR, Proctor A, Hercules DM. Analytical Chemistry 1995;67:1034–41.

[35] Perera IK, Perkins J, Kantartzoglou S. Rapid Communications in Mass Spectrometry 1995;9:180–7.
[36] Vorm O, Roepstorff P, Mann M. Analytical Chemistry 1994;66:3281–7.
[37] Wei H, Nolkrantz K, Powell DH, Woode JH, Ko M-C, Kennedy RT. Rapid Communications in Mass Spectrometry 2004;18:1193–200.
[38] Axelsson J, Scrivener E, Haddleton DM, Derrick PJ. Macromolecules 1996;29:8875–82.
[39] Hanton SD, Hyder IZ, Stets JR, Owens KG, Blair WR, Guttman M, et al. Journal of the American Society for Mass Spectrometry 2004;15:168–79.
[40] Wetzel SJ, Guttman CM, Flynn KM. Rapid Communications in Mass Spectrometry 2004;18:1139–46.
[41] Bruins AP. Journal of Chromatography A 1998;794:345–57.
[42] Chaffey-Millar H, Stenzel MH, Davis TP, Coote ML, Barner-Kowollik C. Macromolecules 2006;39:6406–19.
[43] Jackson AT, Bunn A, Priestnall IM, Borman CD, Irvine DJ. Polymer 2006;47:1044–54.
[44] Borman CD, Jackson AT, Bunn A, Cutter AL, Irvine DJ. Polymer 2000;41:6015–20.
[45] Schon F, Hartenstein M, Muller AHE. Macromolecules 2001;34:5394–7.
[46] Bednarek M, Biedron T, Kubisa P. Macromolecular Rapid Communications 1999;20:59–65.
[47] Datta H, Bhowmick AK, Singha NK. Macromolecular Symposia 2006;240:245–51.
[48] The highlighted m/z ranges of the MALDI and ESI spectra are not identical as these ranges factor in the differing preferential cation attachment observed using the two ionisation modes.
[49] The labelled "peaks" referred to throughout this publication are more correctly clusters of isotopomer ion peaks arising from a common product.
[50] The normal scan types of the LCQ Deca ion trap instrument are contrasted with the *ZoomScan* scan type, which employs a slower scan rate and has higher than normal resolution. Typical mass resolving power and mass accuracy values obtained from the present study are 1800 FWHM and >200 ppm respectively for the normal scan type, and 5700 FWHM and <80 ppm respectively for the *ZoomScan* scan type.
[51] This column states the m/z of the most abundant isotope of the labelled adduct species. As all of the adducts featured in this table contain at least two bromine atoms and thus display isotopic peak patterns in which the lowest mass isotopes are never the most abundant, the listed m/z do not reflect the exact masses of these ions.
[52] This columns lists the S/N of the most abundant isotope signal obtained within the full available m/z range from the adduct species in question.
[53] The bracketed figures represent the S/N data obtained from *ZoomScan* spectra.
[54] This column states the DP_n of all oligomeric/polymeric products corresponding to the adduct species in question which are observed within the full available m/z scan range.
[55] The bracketed figures represent the S/N data obtained from *ZoomScan* spectra. These figures do not necessarily represent the optimal S/N levels possible for the adducts in question, as many of these spectra were taken over m/z ranges in which the adducts were not detected at their most abundant levels.
[56] Van Renterghem LM, Lammens M, Dervaux B, Viville P, Lazzaroni R, Du Prez FE. Journal of the American Chemical Society 2008;130:10802–11.
[57] Zeldes H, Livingston R. The Journal of Chemical Physics 1966;45:1946–54.
[58] Walker DC. The Canadian Journal of Chemistry 1990;68:1719–24.
[59] Pieck R, Steacie EWR. The Canadian Journal of Chemistry 1955;33:1304–15.
[60] Taha IAI, Kuntz RR. The Journal of Physical Chemistry 1969;73:4406–9.
[61] The ability of an instrument to detect products within a given polymer sample is related to the MS technique's detection limit; however, this is not equivalent to the ability for an instrument to detect lower abundance species within a given sample. Though an instrument may be capable of identifying analyte molecules up to a specified detection limit, this detection limit may not necessarily reflect the ability to detect certain species when they are in the presence of more abundant analyte molecules.